

# Inflammatory Responses to Amyloidosis in a Transgenic Mouse Model of Alzheimer's Disease

Yasuji Matsuoka,\* Melanie Picciano,\*  
Brian Malester,\* John LaFrancois,\* Cindy Zehr,<sup>†</sup>  
JoAnna M. Daeschner,<sup>‡</sup> John A. Olschowka,<sup>‡</sup>  
Maria I. Fonseca,<sup>§</sup> M. Kerry O'Banion,<sup>‡</sup>  
Andrea J. Tenner,<sup>§</sup> Cynthia A. Lemere,<sup>¶</sup> and  
Karen Duff\*

From the Dementia Research Group,\* Nathan Kline Institute/New York University Medical Center, Orangeburg, New York; the Mayo Clinic,<sup>†</sup> Jacksonville, Florida; the Department of Neurobiology and Anatomy,<sup>‡</sup> University of Rochester Medical Center, Rochester, New York; the Department of Molecular Biology and Biochemistry,<sup>§</sup> University of California, Irvine, California; and the Center for Neurologic Diseases,<sup>¶</sup> Brigham and Women's Hospital, Harvard Institutes of Medicine, Boston, Massachusetts

**Mutations in the amyloid precursor protein (APP) and presenilin-1 and -2 genes (PS-1, -2) cause Alzheimer's disease (AD). Mice carrying both mutant genes (PS/APP) develop AD-like deposits composed of  $\beta$ -amyloid ( $A\beta$ ) at an early age. In this study, we have examined how  $A\beta$  deposition is associated with immune responses. Both fibrillar and nonfibrillar  $A\beta$  (diffuse) deposits were visible in the frontal cortex by 3 months, and the amyloid load increased dramatically with age. The number of fibrillar  $A\beta$  deposits increased up to the oldest age studied (2.5 years old), whereas there were less marked changes in the number of diffuse deposits in mice over 1 year old. Activated microglia and astrocytes increased synchronously with amyloid burden and were, in general, closely associated with deposits. Cyclooxygenase-2, an inflammatory response molecule involved in the prostaglandin pathway, was up-regulated in astrocytes associated with some fibrillar deposits. Complement component 1q, an immune response component, strongly colocalized with fibrillar  $A\beta$ , but was also up-regulated in some plaque-associated microglia. These results show: i) an increasing proportion of amyloid is composed of fibrillar  $A\beta$  in the aging PS/APP mouse brain; ii) microglia and astrocytes are activated by both fibrillar and diffuse  $A\beta$ ; and iii) cyclooxygenase-2 and complement component 1q levels increase in response to the formation of fibrillar  $A\beta$  in PS/APP mice. (*Am J Pathol* 2001, 158:1345–1354)**

Alzheimer's disease (AD) is characterized clinically by a dementia of insidious onset and pathologically by the

presence of numerous neuritic plaques and neurofibrillary tangles.<sup>1,2</sup> The plaques are composed mainly of  $\beta$ -amyloid ( $A\beta$ ) peptide fragments, derived from processing of the amyloid precursor protein (APP). Tangles consist of paired helical filaments composed of the microtubule-associated protein, tau.<sup>2,3</sup> Transgenic mice carrying a pathogenic mutation in APP (APP<sub>K670N,M671L</sub>) show marked elevation of  $A\beta$ -protein level and  $A\beta$  deposition in the cerebral cortex and hippocampus<sup>4</sup> from approximately 1 year of age. Mutant PS-1 transgenic mice do not show abnormal pathological changes, but do show subtly elevated levels of the  $A\beta$ 42/43 peptide.<sup>5</sup> Transgenic mice derived from a cross between these mice (PS/APP) show markedly accelerated accumulation of  $A\beta$  into visible deposits compared with APP singly transgenic mice.<sup>6</sup> The PS/APP mouse, therefore, has considerable utility in the study of the amyloid phenotype of AD.

It has now been well demonstrated that immune and inflammatory responses can take place in the central nervous system (CNS) as well as the periphery,<sup>7</sup> and that microglia can be considered to be a brain macrophage. Resting microglia exist in a resident (ramified) form characterized by long, thin processes, but on activation, the morphology changes to an amoeboid form, with short, thick processes.<sup>8</sup> Astrocytes also undergo activation in the CNS, and both glial types produce inflammatory-response proteins such as interleukins (ILs), tumor necrosis factor, nitric oxide synthase, cyclooxygenase, and complement proteins. Such immune and inflammatory responses in the CNS are observed in several chronic and acute neurodegenerative diseases including AD, Parkinson's disease, amyotrophic lateral sclerosis, multiple sclerosis, and stroke.<sup>9,10</sup>

To examine how glial cells in the CNS of the PS/APP mouse respond to  $A\beta$  accumulation, we correlated  $A\beta$  deposition with the activation of glial cells (microglia and astrocytes) and the up-regulation of cyclooxygenase-2 (COX-2) and complement component 1q (C1q).

Supported by National Institutes of Health grants NIH AG-16573 (to A. J. T.), NIH AG-172116 (to K. D.), and NS 33553 (to M. K. O.).

Accepted for publication January 12, 2001.

Address reprint requests to Karen Duff, Ph.D., Nathan Kline Institute/New York University, 140 Old Orangeburg Road, Orangeburg, NY 10962. E-mail: duff@nki.rfmh.org.

## Materials and Methods

### Animals and Materials

Mice expressing mutant APP<sub>K670N,M671L</sub> (mutant APP, Tg2576)<sup>4</sup> and mutant PS1<sub>M146L</sub> (mutant PS1, line 6.2)<sup>5</sup> were crossed to generate the PS/APP line. The mice used in this study were 3, 7, 12, 18, and 30 months old ( $n \geq 3$  at each age). For the COX-2 study we used 7- and 12-month-old mice ( $n = 3$ ). For the C1q study, we used 7-, 12-, 14-, and 18-month-old mice (total  $n = 4$ ), and two of the mice were subjected to the double labeling study with the microglia marker.

The following antibodies were used in this study. Rat anti-mouse CD11b, also known as Mac-1  $\alpha$  chain (clone M1/70.15) (Caltag Laboratories, San Francisco, CA); rat anti-F4/80 (Serotec, Raleigh, NC); mouse anti-gliar fibrillary acidic protein (GFAP; clone G-A-5) (Roche Diagnostics, Indianapolis, IN); mouse anti-human A $\beta$  residues 17–24 (clone 4G8) (Senetek, Maryland Heights, MO); rabbit anti-murine COX-2 (Cayman Chemical, Ann Arbor, MI); rabbit anti-GFAP (for human immunohistochemistry; Dako, Carpinteria, CA).

Polyclonal antibodies against human A $\beta$ , C40 and C42, were kind gifts from Dr. Saido (RIKEN Brain Institute, Saitama, Japan). C40 and C42 were developed using synthetic A $\beta$  peptide residue 36–40 and 38–42, respectively, as an antigen, and are specific for A $\beta$  ending at residue 40 and 42, respectively.<sup>11</sup> Goat anti-mouse C1q antibody was a kind gift from Dr. F. Petry (Institute of Medical Microbiology and Hygiene, Johannes-Gutenberg University, Mainz, Germany).<sup>12</sup>

### Immunohistochemistry

The animals were perfused through the left cardiac ventricle with 10 ml of cold 10 mmol/L phosphate-buffered saline (PBS), pH 7.4, under deep anesthesia, followed by 40 ml of a cold fixative consisting of 4% paraformaldehyde in 100 mmol/L phosphate buffer, pH 7.4. After perfusion, the brain was quickly removed and postfixed for 18 hours with the same fixative at 4°C, and 30- $\mu$ m-thick frozen sections were prepared using a freezing microtome (Physitemp, Clifton, NJ, and Leica, Heidelberg, Germany). Free-floating sections were treated with 0.3% hydrogen peroxide in 100 mmol/L PBS containing 0.3% Triton-X 100 (PBST) for 30 minutes, and nonspecific protein binding was blocked by incubation with 10% normal goat serum in PBST for 1 hour. Sections were incubated with primary antibodies against A $\beta$  (333 ng IgG/ml), CD11b (1  $\mu$ g IgG/ml), and GFAP (20 ng IgG/ml) overnight at room temperature. Primary antibodies were detected by biotinylated secondary antibodies (1.5  $\mu$ g IgG/ml each, Vector Laboratories, Burlingame, CA) and visualized by the ABC method (ABC Elite kit, Vector Laboratories). After each incubation, sections were rinsed in PBST 3 times for 10 minutes each.

For COX-2 immunohistochemistry, unfixed frozen brain tissue was cut at 18  $\mu$ m using a sledge microtome, mounted onto slides, and fixed in 4% paraformaldehyde for 10 minutes. Slides were washed in 150 mmol/L phos-

phate buffer, and antigen retrieval was performed in 100% cold methanol for 10 minutes.<sup>13</sup> After rehydration, sections were blocked with normal goat serum, then incubated with anti-COX-2 antibody (1:500). COX-2 antibody was detected as described above. For double labeling, sections were incubated with primary antibodies against COX-2 and GFAP, then visualized with Alexa Fluor 488- or 588-labeled secondary antibodies (Molecular Probes, Eugene, OR). Fluorescent images were captured using a Zeiss Axioplan microscope equipped with a Spot II digital camera and software (Diagnostic Instruments Inc., Sterling Heights, MI).

For C1q immunostaining, sections were incubated for 1 hour with 2% bovine serum albumin and 1% normal rabbit serum in Tris-HCl buffer (pH 7.4) containing 0.1% Triton X-100, and then incubated with anti-C1q antibody (7  $\mu$ g/ml) overnight at 4°C. Antibody was detected by the ABC method. For double immunolabeling of C1q and a marker for microglia, C1q was first detected by FITC-labeled anti-goat Ig (1:500, Jackson Immunoresearch, West Grove, PA) and photographed. Sections were washed and then stained with F4/80 (1:50). Label was detected with biotinylated secondary and ABC method as above.

Immunohistochemistry on human brain was performed as described previously.<sup>14</sup> Primary antibodies were used at dilutions of 1:500 (C40 and C42) or 1:1000 (GFAP).

To clarify the association between fibrillar A $\beta$  and a specific antigen, immunostained sections were mounted on glass slides and incubated with 1% thioflavin-S (Sigma, St. Louis, MO) in 70% ethanol for 20 minutes, then rinsed with 70, 95, and 100% ethanol. Thioflavin-S was visualized using a specific filter set (excitation, 405–445 nm; emission, 515–565 nm).

Amyloid burden was assessed according to the method of Takeuchi et al.<sup>15</sup> In brief, the percentage of the frontal cortex covered by 4G8-immunoreactivity or thioflavin-S, was assessed on consecutive sections from 3 separate mice using MCID image analysis software (Imaging Research, St. Catharines, ON).

## Results

### Increase of A $\beta$ with Aging

Mice younger than 3 months of age initially deposit A $\beta$  in the frontal cortex (Figure 1A) as visualized with anti-A $\beta$  antibody (4G8). Visible deposits were not seen in more caudal regions at this age (Figure 1B). As the animals aged, A $\beta$  deposition spreads throughout the cortex, and to the hippocampus, thalamus, and amygdala (Figure 1C). By 1 year of age, A $\beta$  deposits were widely observed, but there was not a marked change in the total amount of amyloid deposited beyond that age (Figure 1, D–F). A second monoclonal antibody that recognizes A $\beta$  residues 1–17 (6E10) showed essentially the same distribution pattern (data not shown). For our purposes, 4G8 was considered to recognize total A $\beta$  as it recognizes both diffuse and fibrillar A $\beta$ .

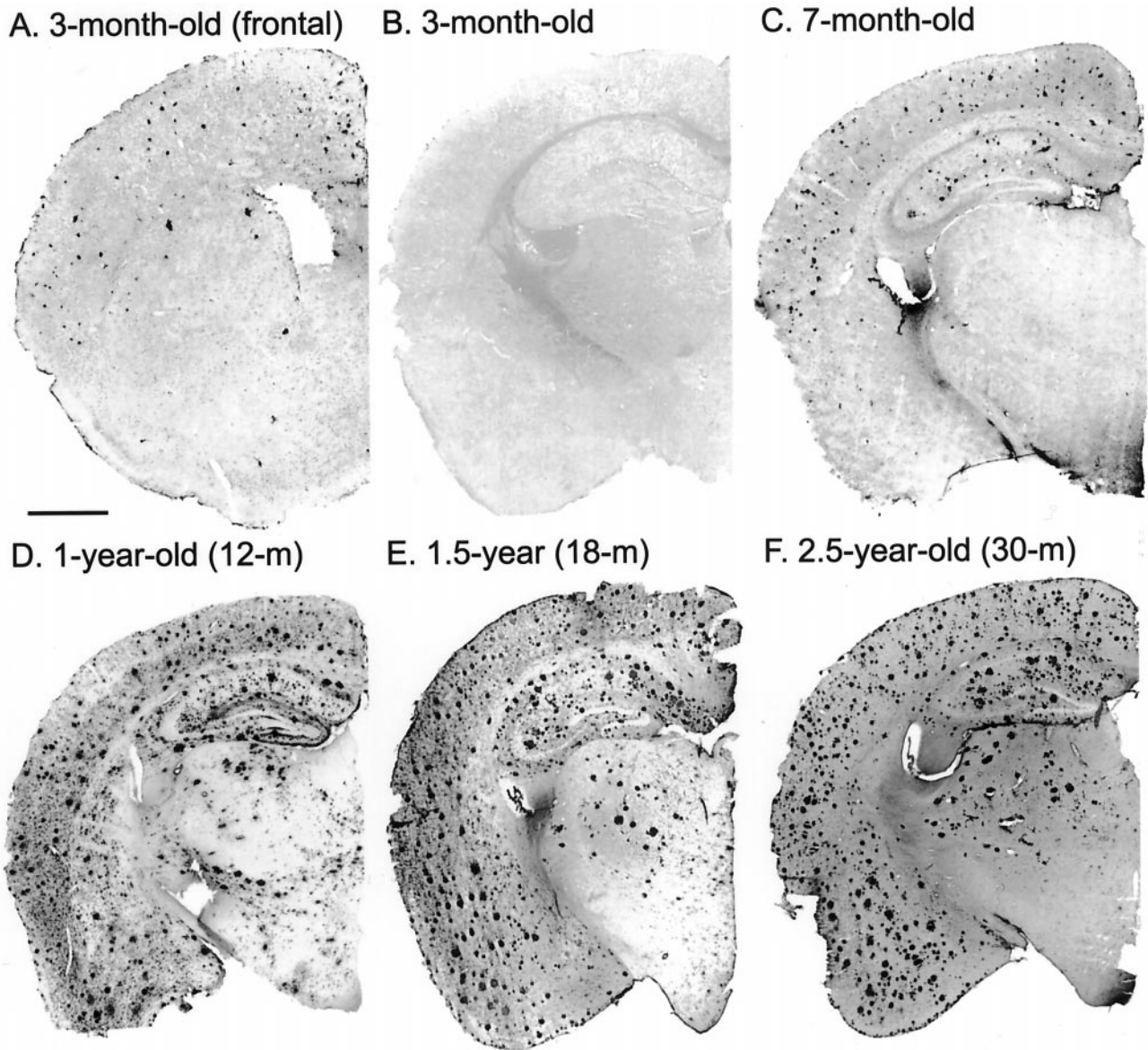


**Figure 1.** In a longitudinal aging study of PS/APP transgenic mice, A $\beta$  load and distribution were compared in the cerebral cortex, at the level of the amygdala (except **A**) using antibody 4G8. A $\beta$  deposition in mice younger than 3 months of age was initiated in the frontal cortex (**A**), but at this age, A $\beta$  deposits were not visible elsewhere (**B**). By 7 months of age, A $\beta$  deposition in the cerebral cortex and the hippocampus had increased extensively (**C** and **D**). After approximately 1 year of age, the total amyloid load remained more consistent (**E** and **F**). Scale bar, 1 mm.

A few fibrillar A $\beta$  deposits were also detected in the frontal cortex of the youngest mice (Figure 2A), but they were absent from more caudal regions (Figure 2B). The number of fibrillar A $\beta$  deposits increased synchronously with an increase in total A $\beta$  up to 1 year of age, although fibrillar A $\beta$  deposits were fewer and smaller than 4G8 immunoreactive total A $\beta$  deposits in the brains of younger animals (Figure 1, A–D, vs. Figure 2, A–D). Fibrillar A $\beta$  increased markedly after 1 year of age (Figure 2, D–F), although total A $\beta$  levels remained relatively consistent. The relative amount of total and fibrillar A $\beta$  was quantified (Figure 3). The area covered by total A $\beta$  increased markedly up to 1 year of age, but the levels did not show a marked change at older ages (Figure 3, open column and continuous line). In contrast, the area covered by fibrillar A $\beta$  increased consistently up to 2 years of age

(Figure 3, closed column and dotted line). At 1 year of age, the percentage of brain covered by fibrillar A $\beta$  ( $15 \pm 2\%$ ) was approximately half that covered by total A $\beta$  ( $29 \pm 5\%$ ), but by 2.5 years of age, fibrillar A $\beta$  ( $32 \pm 4\%$ ) accounts for almost all of the 4G8-immunoreactive A $\beta$  present ( $33 \pm 2\%$ ) in the brain.

#### *Activation of Glial Cells in PS/APP Transgenic Mice*

Activated microglia accumulated around A $\beta$  deposits (Figure 4F) from the earliest age at which they were visible (approximately 3 months), and the number increased synchronously with age and increased amyloid burden (Figure 4, B–E). Very few activated CD11b-immu-

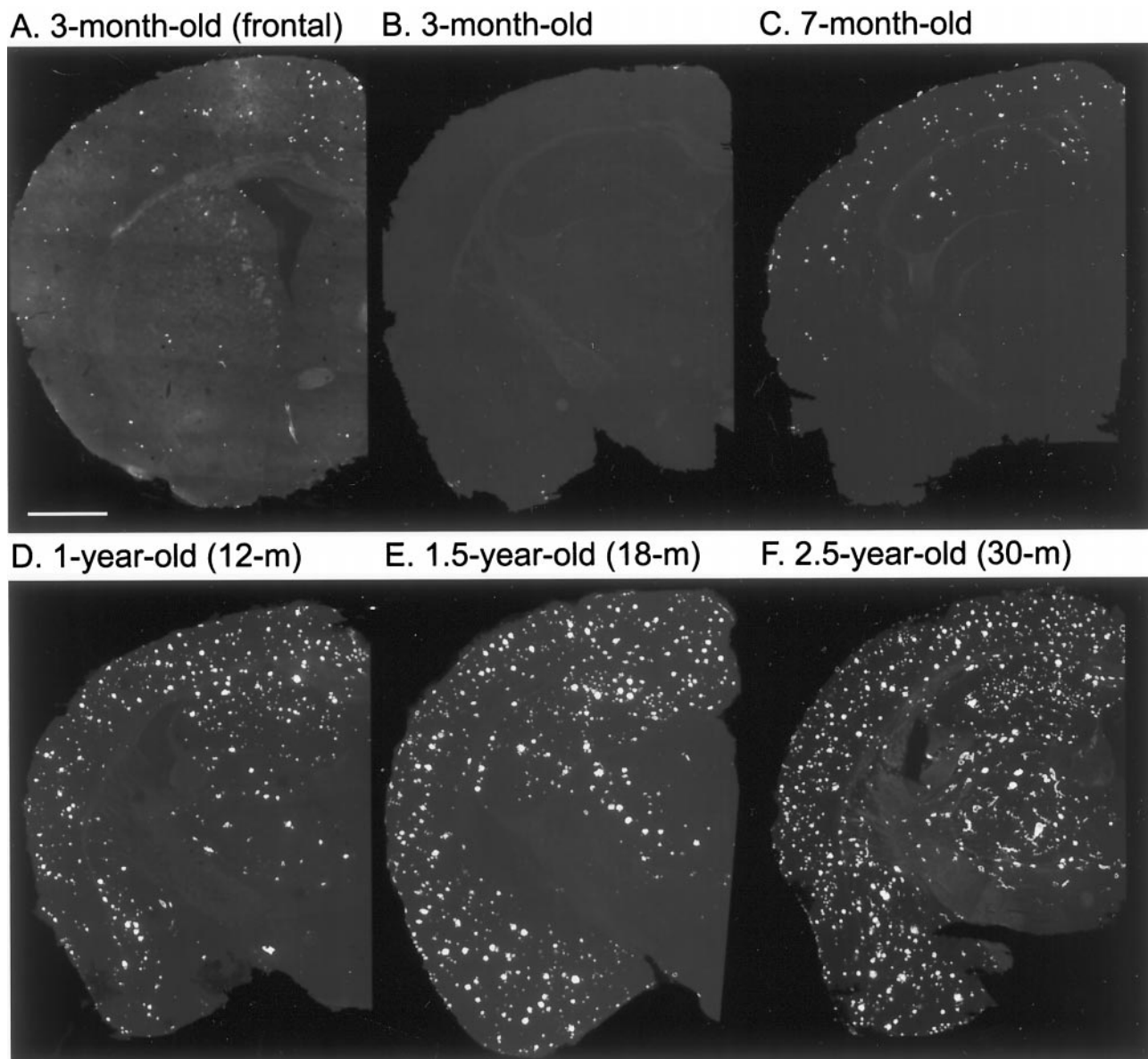


**Figure 2.** Fibrillar A $\beta$  as detected by thioflavin-S staining in aging PS/APP transgenic mice was compared in sections taken from the level of the amygdala (except A). Fibrillar A $\beta$  was identified in the frontal cortex of the youngest mice studied, and it increased with total A $\beta$  in aged animals (D–F). Scale bar, 1 mm.

noreactive microglia were observed in regions of the brain (Figure 4A) where visible amyloid deposits had not yet developed (Figure 2A). Neither amyloid deposits nor activated microglia were observed in nontransgenic littermate animals using these staining protocols (data not shown).

To examine the association of activated microglia with diffuse (thioflavin-S-negative) A $\beta$  and fibrillar (thioflavin-S-positive) A $\beta$  deposits, serial sections were stained with anti-A $\beta$  antibody (4G8; Figure 5A) and anti-CD11b antibody (Figure 5B). After immunostaining, sections were counterstained with thioflavin-S (Figure 5C). CD11b-immunoreactive activated microglia associated with both diffuse and fibrillar A $\beta$  deposits (Figure 5).

GFAP-immunopositive reactive astrocytes were not observed in nontransgenic animals (data not shown). Reactive astrocytes were first observed in association

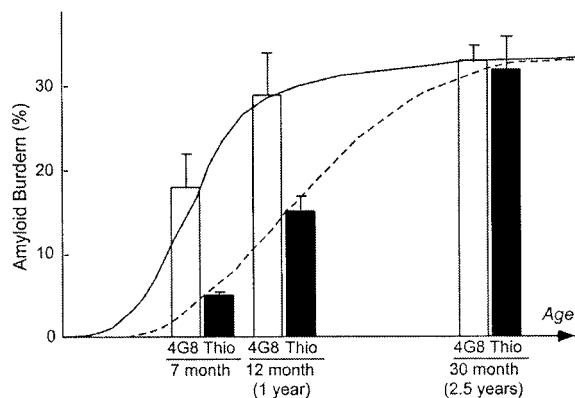


**Figure 3.** Quantitative analysis of amyloid burden in the cortex. The percentage of the frontal cortex area covered by 4G8 immunoreactivity (total A $\beta$ , both fibrillar and diffuse A $\beta$ ) or thioflavin-S (fibrillar A $\beta$  only) (open and closed columns, respectively) was measured. Data are presented as mean  $\pm$  SE ( $n = 3$ ).

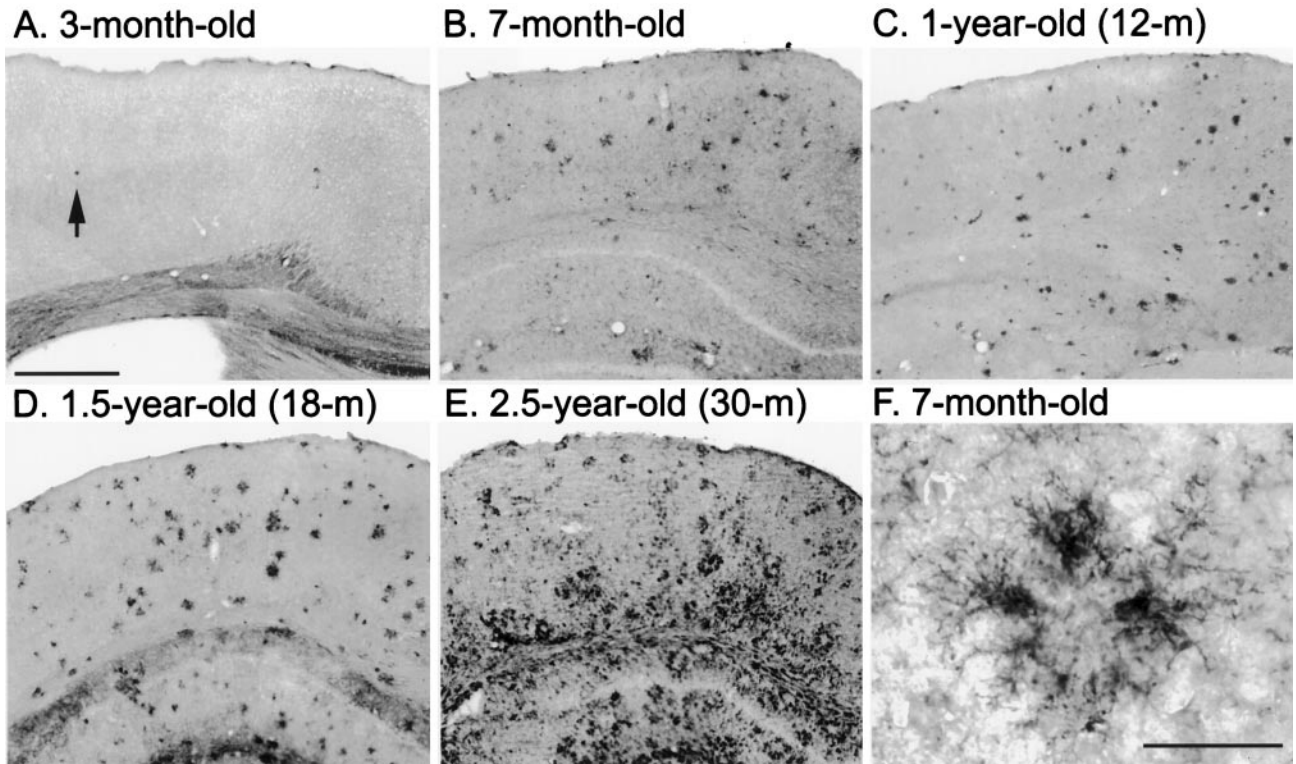


**Figure 4.** The activation of microglia in response to amyloid accumulation was compared in the frontal cortex of PS/APP mouse brains. A few CD11b-immunoreactive activated microglia were observed at 3 months of age (A), and the numbers increased with increasing amyloid burden and age (B–E). Activated microglia were observed surrounding A $\beta$  deposits at all ages (F), although more generalized gliosis was also seen in older mice (E). Scale bars, 500  $\mu$ m (in A for A–E) and 40  $\mu$ m (F).

with amyloid deposits in the frontal cortex of 3-month-old PS/APP mice (Figure 6A), but they were very rarely seen in regions of the brain devoid of accumulated amyloid (Figure 6B). By 7 months of age, GFAP-immunoreactive astrocytes were abundant and closely associated with A $\beta$  deposits throughout the brain (Figure 6, C and G). As the animals aged, astrocytosis and amyloidosis increased in parallel except in some regions of the cortex of older animals, where the astrocytes appeared dystrophic and no longer closely associated with the plaque (Figure 6, E, F, and H). This has also been seen occasionally around very compacted plaques in late stage

human AD brain, as shown in Figure 7. This figure shows sections from the temporal cortex of an early onset familial AD (FAD) patient carrying the E280A *PS-1* mutation who has very advanced AD pathology.<sup>14</sup> The figure shows a plaque that is devoid of GFAP-reactive astrocytes (Figure 7, D–F), lying close to plaques that are still associated with reactive astrocytes (Figure 7, A–C). This type of pathology around burned-out plaques has been observed in several FAD and non-FAD brains, although it is rare (approximately 2 to 5% of very compact, cortical plaques in FAD brains lack an association with GFAP-immunopositive astrocytes; CA Lemere, unpublished

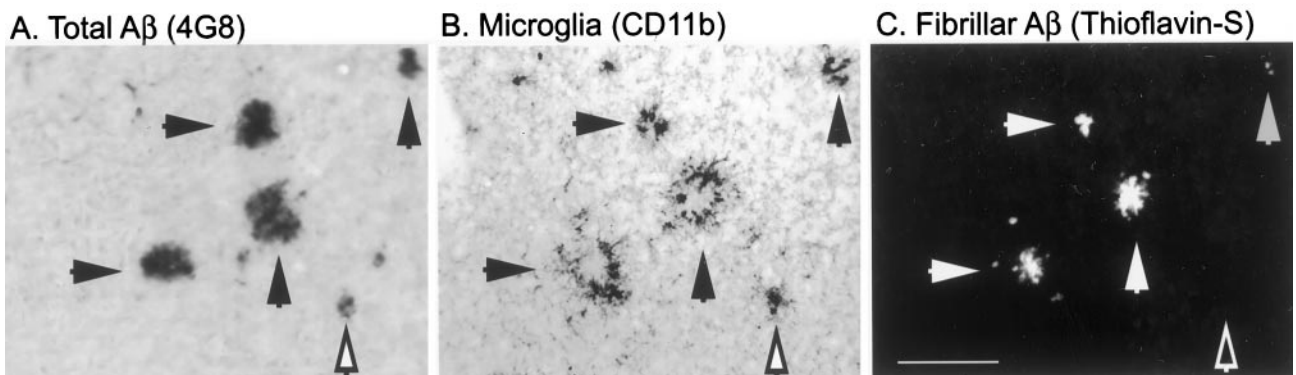
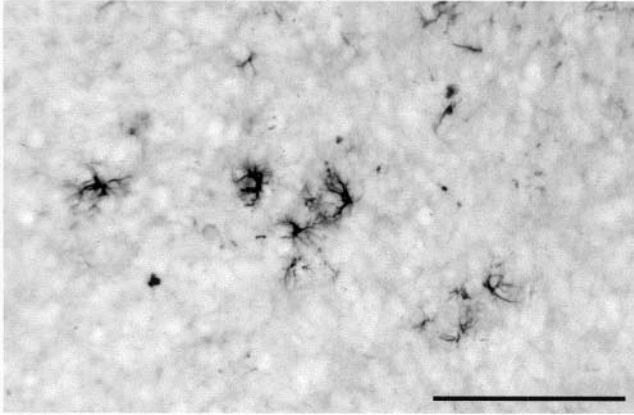
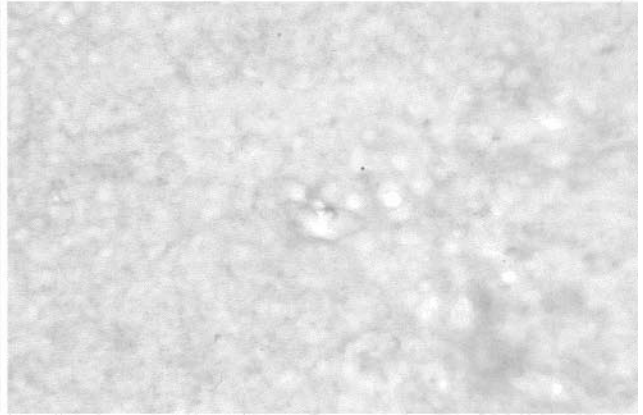


**Figure 5.** Association of activated microglia with fibrillar and nonfibrillar A $\beta$  deposits in 7-month-old PS/APP mouse brain. Two serial sections were stained with anti-A $\beta$  antibody (4G8) (A) and CD11b antibodies (B). CD11b-immunostained section were then counterstained with thioflavin-S to detect fibrillar A $\beta$  (C). CD11b-immunoreactive activated microglia colocalize with both fibrillar A $\beta$  (closed arrows) and thioflavin-S negative (but 4G8 positive) A $\beta$  deposits (open arrow). Scale bar, 100  $\mu$ m.

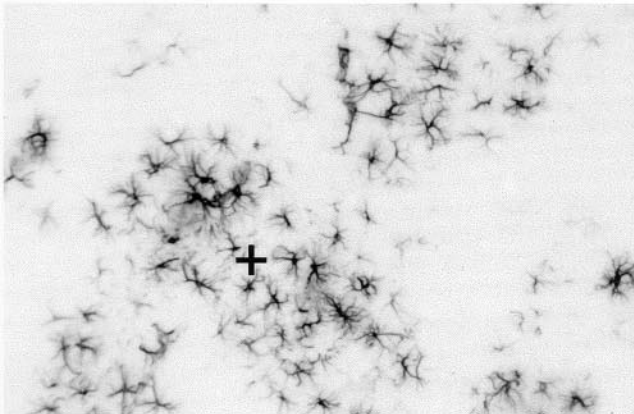
**A. 3-month-old (frontal)**



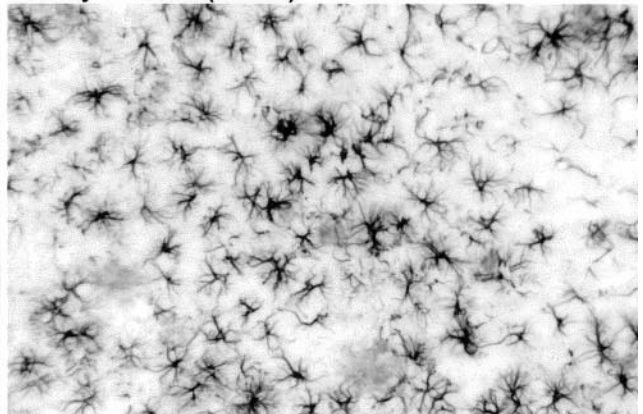
**B. 3-month-old**



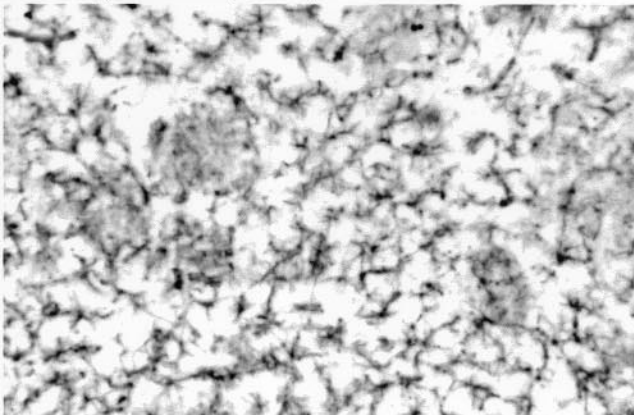
**C. 7-month-old**



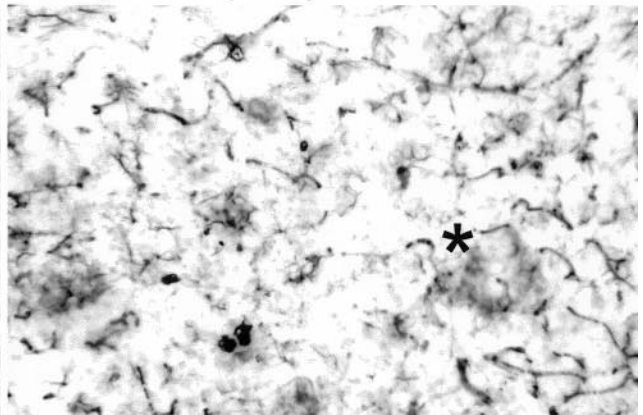
**D. 1-year-old (12-m)**



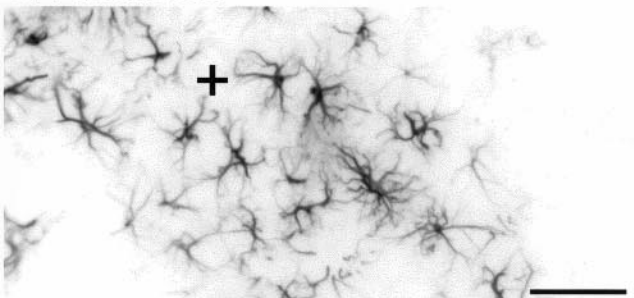
**E. 1.5-year-old (18-m)**



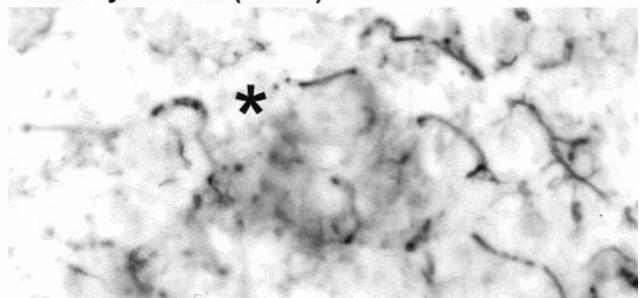
**F. 2.5-year-old (30-m)**



**G. 7-month-old**



**H. 2.5-year-old (30-m)**



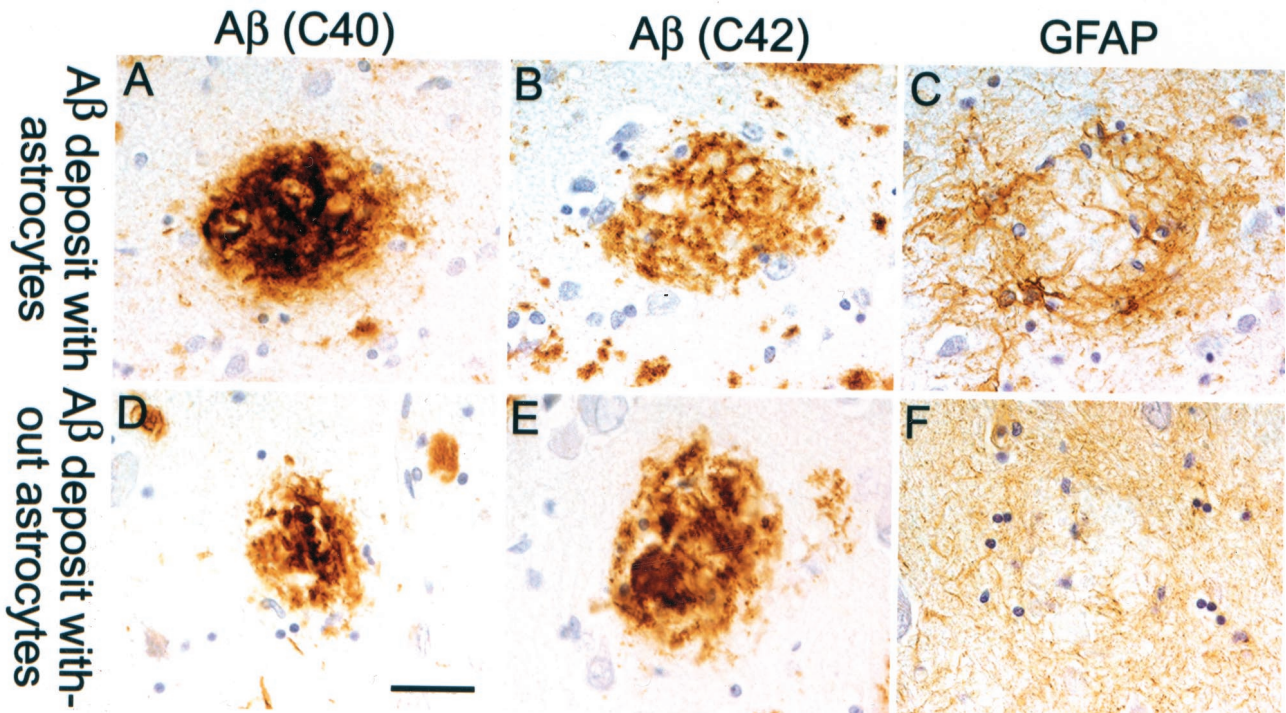


**Figure 7.** Association of GFAP astrocytes with plaques in the temporal cortex of a human patient with late-stage AD. The series on the top (A–C) shows an A $\beta$  plaque immunolabeled with antibodies against A $\beta$ 40 and A $\beta$ 42, respectively (A and B) surrounded by a cluster of reactive astrocytes (C). Bottom panels (D–F) show an A $\beta$  plaque (D and E) which lacks reactive astrocyte cell bodies; however, there is a general meshwork of weakly stained astrocytic processes (F). All panels in this figure were taken from the same section. The sections were counterstained with hematoxylin so that the nuclei stained purple. Scale bar, 50  $\mu$ m.

data). We have now observed this type of astrocyte pathology in the cerebral cortex of more than five PS/APP mice aged 12 to 18 months that have had extensive and protracted amyloid accumulation.

#### Induction and Colocalization of COX-2

COX-2 expression was observed in neurons in the brains of both transgenic (Figure 8B) and nontransgenic mice (data not shown). In the brains of PS/APP mice, COX-2 expression was also identified in glial cells associated with A $\beta$  deposits (Figure 8A), however, many deposits (including thioflavin-S-positive fibrillar A $\beta$  deposits) were not associated with COX-2 immunoreactive cells. Double immunostaining with COX-2 and GFAP confirmed the astrocytic phenotype of the plaque-associated COX-2 immunoreactive cells (Figure 8A, inset).

#### Colocalization of C1q

In the four PS/APP mice studied, C1q-immunoreactivity colocalized with thioflavin-S positive fibrillar A $\beta$  (Figure 9A and D, B and E) and was also identified in cells associated with plaques. Double immunostaining with a

microglial marker (F4/80) and C1q shows that in the PS/APP mouse brain, C1q colocalizes with activated microglia (Figure 9, C and F). We did not observe neuronal staining of C1q in the PS/APP mice examined, nor was immunoreactivity observed in nontransgenic littermates (data not shown).

#### Discussion

One of the most significant pathological features in AD is the accumulation of A $\beta$  peptides and their deposition into plaques. Doubly transgenic mice carrying mutant *PS-1* and *APP* transgenes show a rapid accumulation of both fibrillar and diffuse forms of A $\beta$ <sup>6</sup> from 10 to 12 weeks of age up to the oldest age studied, 2.5 years. To date, neurofibrillary pathology in the PS/APP mouse has been limited to enhanced phospho-tau immunoreactivity in dystrophic neurites surrounding the deposits.<sup>15</sup> The lack of extensive neurofibrillary pathology has allowed us to examine the effects of increasing amyloid burden on surrounding cellular responses relevant to AD.

In the PS/APP mice, nonfibrillar amyloid accumulates to a greater extent in the initial deposition period, but at

**Figure 6.** The activation of plaque-associated astrocytes in the cerebral cortex of PS/APP mice was compared on sections taken at the level of the amygdala (except A). A few activated astrocytes were observed in the vicinity of plaques in the frontal cortex of 3-month-old mice (A), but they were absent from regions devoid of visible A $\beta$  deposits (B). Up to approximately 1 year of age, GFAP-immunoreactive astrocytes were strongly associated with plaques (C and D). In older mice, A $\beta$ -related astrocytosis was extensive except in certain regions of the cortex where the cell bodies and processes appeared more dystrophic or weakly stained (E and F). G and H: GFAP-immunoreactive astrocytes around plaques in the cortex of a 7-month-old mouse (G) and a 2.5-year-old mouse (H). E, F, and H have some background staining on A $\beta$  deposits. Markers (+ and \*) indicate the same region in C and G and in F and H, respectively. Scale bars, 200  $\mu$ m (in A for A–F) and 50  $\mu$ m (in G for G and H).

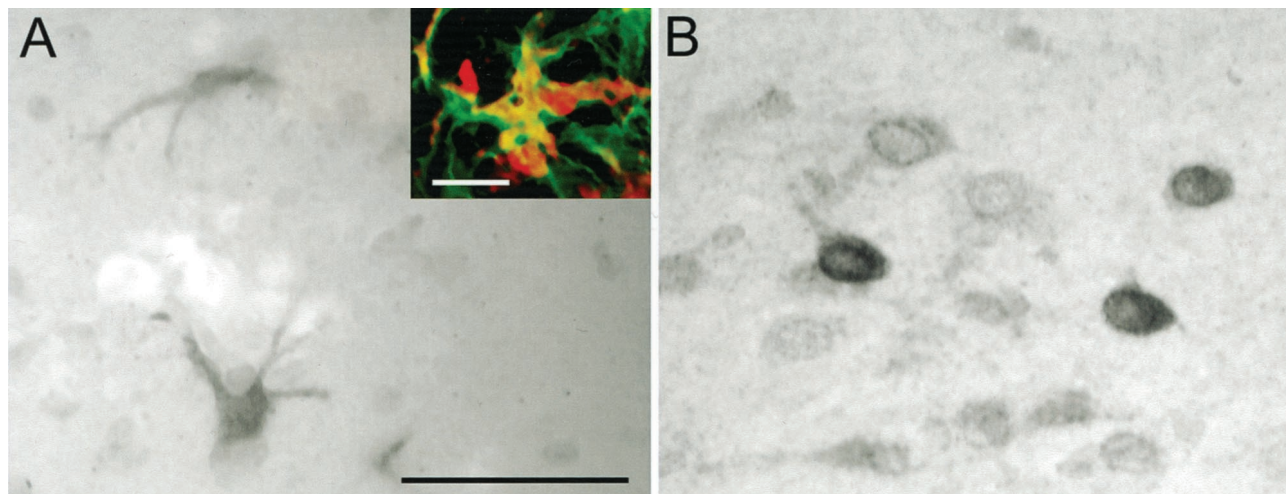


**Figure 8.** Induction of COX-2 and its association with A $\beta$  in 7-month-old PS/APP brain (**A**). Double labeling with COX-2 (red) and GFAP (green) demonstrate colocalization (yellow; **A, inset**) in astrocytes around plaques. Neuronal COX-2 expression is observed in PS/APP brain (**B**) as well as in nontransgenic mouse brain (data not shown).

later stages (after 1 year of age) fibrillar forms are increasingly represented. CD11b, a 170-kd integrin  $\alpha_M$  chain protein (also referred to as a Mac-1  $\alpha$  chain), and GFAP are specific markers for activated microglia and astrocytes, respectively. Activated microglia (CD11b-immunoreactive) and astrocytes (GFAP-immunoreactive) were colocalized with amyloid deposits, as has also been shown in other transgenic models of amyloidosis.<sup>16</sup> Both diffuse and fibrillar deposits were associated with activated astrocytes and microglia. In human AD brain, approximately half of the diffuse (nonfibrillar) deposits had

no activated microglia associated with them, and a large percentage of the remainder had single microglia colocalized with the diffuse plaques. In contrast, nearly all compact deposits had single or multiple activated microglia embedded in their core.<sup>17,18</sup> The transgenic mouse models have plaque morphologies more closely representing compact, dense cores, which may explain why more plaques are associated with glial reactivity. In aged PS/APP mice, the association of reactive astrocytes with deposits in some regions of the cortex is diminished. Whether this population of plaques represent the type of

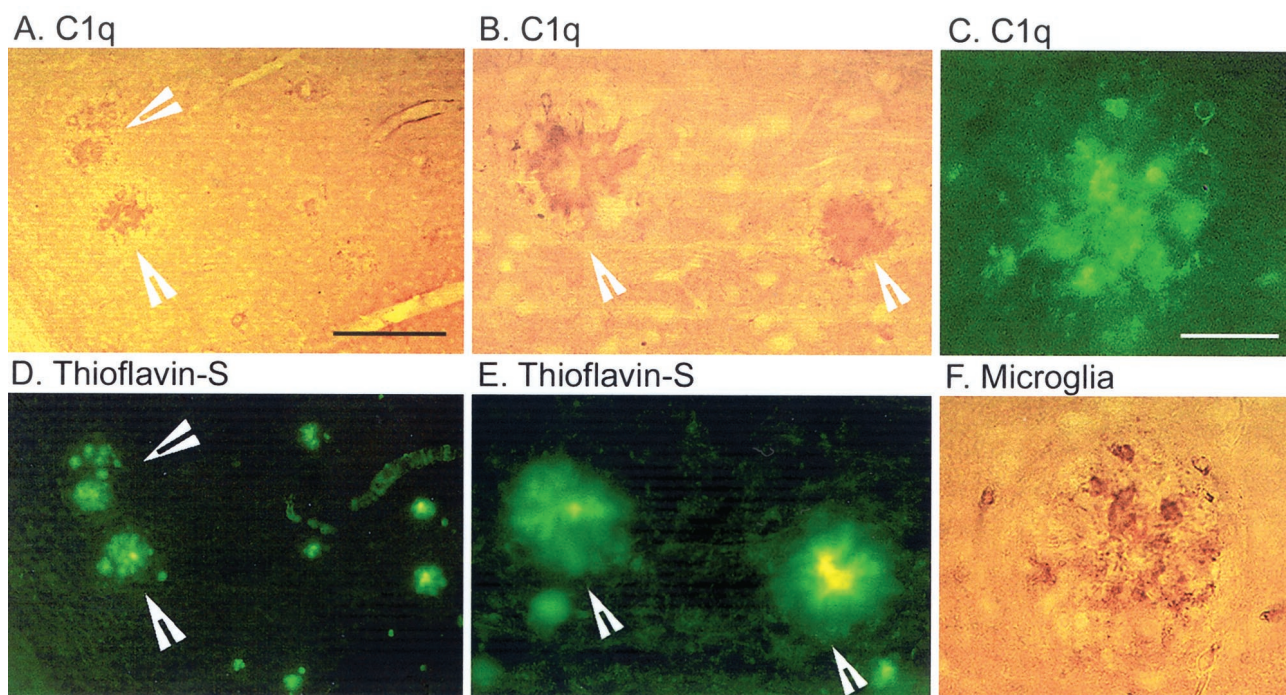


**Figure 9.** Colocalization of C1q with fibrillar A $\beta$  plaques and associated microglia in 12- (**A** and **D**) or 7-month-old (**C** and **F**) PS/APP mouse brain. C1q-immunostained sections were counterstained with thioflavin-S to detect fibrillar A $\beta$ . To examine the cellular location of C1q, one section was incubated sequentially with fluorescently labeled C1q (**C**) and F4/80 (**F**) which was then detected with DAB. C1q appears to colocalize both with plaques and with microglia. Scale bars, 50  $\mu$ m (in **A** for **A, B, D,** and **E**) and 25  $\mu$ m (in **C** for **C** and **F**).



burned-out plaques that lack associated reactive astrocytes seen occasionally in some late stage human AD cases<sup>19</sup> remains to be clarified, and the significance of this type of plaque can only be speculated on.<sup>20–23</sup>

The accumulation of A $\beta$  leads to the activation of several pathways in cells closely associated with the deposits. In the PS/APP mouse, as in human AD brain, C1q is found associated with fibrillar A $\beta$  itself (Figure 9).<sup>20</sup> In PS/APP mice, C1q has also been identified in microglia surrounding some of the deposits. C1q is the first component of the classic complement pathway, and it is possible that induction is evoked for the other members of the pathway (C2–C9) and formation of the membrane-attack complex (MAC), although there are currently few mouse complement-specific antibodies to test this possibility. MAC has been cited as playing a role in neurodegeneration,<sup>21,22</sup> and one possible explanation for why the mice show so little neurodegeneration is that some of the mouse strains that comprise the PS/APP background are complement-insufficient.<sup>23</sup> The presence of C1q suggests that the mice are able to mount an inflammatory response to A $\beta$  that would result in the formation of MAC, although this has not been shown in the mouse as of yet. In addition, the sequence of mouse and human C1q are sufficiently divergent that it has been postulated that mouse C1 will be activated less effectively by fibrillar A $\beta$  than human C1.<sup>24</sup> Although a direct comparison between mouse and human C1 activation has not been performed *in vivo*, it is clear that there is an abundance of mouse C1q in the PS/APP mouse plaques.

The cyclooxygenases catalyze the first step in the conversion of arachidonic acid into prostaglandins (PG), and the resulting PGs have a wide variety of physiological functions.<sup>25–27</sup> Our observation of neuronal COX-2 immunoreactivity in normal and transgenic mouse brain is consistent with observations in other species.<sup>28</sup> Although COX-2 is readily induced in cultured astrocytes and microglia treated with proinflammatory agents and growth factors,<sup>29–32</sup> there are relatively few examples of glial COX-2 expression *in vivo*. Hirst et al<sup>33</sup> showed increased COX-2 immunoreactivity in rat astrocytes following injection of kainic acid, and Tonai et al<sup>34</sup> reported COX-2 immunoreactive astrocytes in rat spinal cord after IL-1 injection. COX-2 immunoreactive microglia have been reported in chronic inflammation associated with a murine prion disease model.<sup>35</sup> To our knowledge, our findings represent the first report of COX-2 immunoreactive glial cells in a murine model of AD. It should be noted, however, that in the human AD brain, up-regulation of COX-2 has been noted in neurons but not in plaque-associated astrocytes. Initial studies suggest there is no gross up-regulation of neuronal COX-2 in plaque-dense areas of the PS/APP mouse brain, but quantitative studies have not yet been performed.

In conclusion, we have studied the inflammatory responses in doubly transgenic mice with abundant amyloid. Our longitudinal studies show that the accumulation of fibrillar A $\beta$  starts at 10 to 12 weeks and continues to increase up to at least 2.5 years of age. Microglia and astrocytes become activated in the presence of aggregated amyloid, leading to profound gliosis in older age.

This progression correlates with activation of the classical complement pathway as shown by the presence of C1q both in plaques, and in activated microglia, and with the activation of the PG pathway as shown by the up-regulation of COX-2 in plaque-associated astrocytes.

## Acknowledgments

We thank Dr. Hsiao-Ashe (Department of Neurology, University of Minnesota, Minneapolis, MN) for the gift of Tg2576 mice, and Dr. Mrak (Department of Pathology, University of Arkansas for Medical Sciences, Little Rock, AK) for critical reading of the manuscript.

## References

1. Hardy J, Duff K, Hardy KG, Perez-Tur J, Hutton M: Genetic dissection of Alzheimer's disease and related dementias: amyloid and its relationship to tau. *Nat Neurosci* 1998, 1:355–358
2. Neve RL, Robakis NK: Alzheimer's disease: a re-examination of the amyloid hypothesis. *Trends Neurosci* 1998, 21:15–19
3. Goedert M: Tau protein and the neurofibrillary pathology of Alzheimer's disease. *Trends Neurosci* 1993, 16:460–465
4. Hsiao K, Chapman P, Nilsen S, Eckman C, Harigaya Y, Younkin S, Yang F, Cole G: Correlative memory deficits, A $\beta$  elevation, and amyloid plaques in transgenic mice. *Science* 1996, 274:99–102
5. Duff K, Eckman C, Zehr C, Yu X, Prada CM, Perez-Tur J, Hutton M, Buee L, Harigaya Y, Yager D, Morgan D, Gordon MN, Holcomb L, Refolo L, Zenk B, Hardy J, Younkin S: Increased amyloid- $\beta$ 42(43) in brains of mice expressing mutant presenilin 1. *Nature* 1996, 383:710–713
6. Holcomb L, Gordon MN, McGowan E, Yu X, Benkovic S, Jantzen P, Wright K, Saad I, Mueller R, Morgan D, Sanders S, Zehr C, O'Campo K, Hardy J, Prada CM, Eckman C, Younkin S, Hsiao K, Duff K: Accelerated Alzheimer-type phenotype in transgenic mice carrying both mutant amyloid precursor protein and presenilin 1 transgenes. *Nat Med* 1998, 4:97–100
7. Friedman EM, Irwin MR: Modulation of immune cell function by the autonomic nervous system. *Pharmacol Therap* 1997, 74:27–38
8. Gonzalez-Scarano F, Baltuch G: Microglia as mediators of inflammatory and degenerative diseases. *Annu Rev Neurosci* 1999, 22:219–240
9. McGeer PL, Kawamata T, Walker DG, Akiyama H, Tooyama I, McGeer EG: Microglia in degenerative neurological disease. *Glia* 1993, 7:84–92
10. McGeer PL, McGeer EG: Glial cell reactions in neurodegenerative diseases: pathophysiology and therapeutic interventions. *Alzheimer Dis Assoc Disord* 1998, 12(suppl 2):S1–S6.
11. Saido TC, Iwatsubo T, Mann DM, Shimada H, Ihara Y, Kawashima S: Dominant and differential deposition of distinct  $\beta$ -amyloid peptide species, A $\beta$  N3(pE), in senile plaques. *Neuron* 1995, 14:457–466
12. Trinder PK, Faust D, Petry F, Loos M: Modulation of mRNA expression and secretion of C1q in mouse macrophages by anti-inflammatory drugs and cAMP: evidence for the partial involvement of a pathway that includes cyclooxygenase, prostaglandin E2 and adenylate cyclase. *Immunology* 1995, 84:638–644
13. O'Banion MK, Olschowka JA: Localization and distribution of cyclooxygenase-2 in brain tissue by immunocytochemistry. *Prostaglandin Protocols*. Edited by Lianos EA. Totowa, NJ, Humana Press, 1999, pp 55–66
14. Lemere CA, Lopera F, Kosik KS, Lendon CL, Ossa J, Saido TC, Yamaguchi H, Ruiz A, Martinez A, Madrigal L, Hincapie L, Arango JC, Anthony DC, Koo EH, Goate AM, Selkoe DJ, Arango JC: The E280A presenilin 1 Alzheimer mutation produces increased A $\beta$  42 deposition and severe cerebellar pathology. *Nat Med* 1996, 2:1146–1150
15. Takeuchi A, Irizarry MC, Duff K, Saido TC, Hsiao AK, Hasegawa M, Mann DM, Hyman BT, Iwatsubo T: Age-related amyloid  $\beta$  deposition in transgenic mice overexpressing both Alzheimer mutant presenilin

- 1 and amyloid  $\beta$  precursor protein Swedish mutant is not associated with global neuronal loss. *Am J Pathol* 2000, 157:331–339
16. Frautschy SA, Yang F, Irrizarry M, Hyman B, Saito TC, Hsiao K, Cole GM: Microglial response to amyloid plaques in APPsw transgenic mice. *Am J Pathol* 1998, 152:307–317
  17. Itagaki S, McGeer PL, Akiyama H, Zhu S, Selkoe D: Relationship of microglia and astrocytes to amyloid deposits of Alzheimer disease. *J Neuroimmunol* 1989, 24:173–182
  18. Cotman CW, Tenner AJ, Cummings BJ:  $\beta$ -Amyloid converts an acute phase injury response to chronic injury responses. *Neurobiol Aging* 1996, 17:723–731
  19. Mrak RE, Sheng JG, Griffin WS: Correlation of astrocytic S100 $\beta$  expression with dystrophic neurites in amyloid plaques of Alzheimer's disease. *J Neuropathol Exp Neurol* 1996, 55:273–279
  20. Griffin WS, Sheng JG, McKenzie JE, Royston MC, Gentleman SM, Brumback RA, Cork LC, Del Bigio MR, Roberts GW, Mrak RE: Life-long overexpression of S100 $\beta$  in Down's syndrome: implications for Alzheimer pathogenesis. *Neurobiol Aging* 1998, 19:401–405
  21. Griffin WS, Sheng JG, Royston MC, Gentleman SM, McKenzie JE, Graham DI, Roberts GW, Mrak RE: Glial-neuronal interactions in Alzheimer's disease: the potential role of a 'cytokine cycle' in disease progression. *Brain Pathol* 1998, 8:65–72
  22. Fonseca MI, Head E, Velazquez P, Cotman CW, Tenner AJ: The presence of isoaspartic acid in beta-amyloid plaques indicates plaque age. *Exp Neurol* 1999, 157:277–288
  23. Mrak RE, Griffin WS: Interleukin-1 and the immunogenetics of Alzheimer disease. *J Neuropathol Exp Neurol* 2000, 59:471–476
  24. Afagh A, Cummings BJ, Cribbs DH, Cotman CW, Tenner AJ: Localization and cell association of C1q in Alzheimer's disease brain. *Exp Neurol* 1996, 138:22–32
  25. McGeer PL, Kawamata T, Walker DG, Akiyama H, Tooyama I, McGeer EG: Microglia in degenerative neurological disease. *Glia* 1993, 7:84–92
  26. Aisen PS, Davis KL: Inflammatory mechanisms in Alzheimer's disease: implications for therapy. *Am J Psych* 1994, 151:1105–1113
  27. Ong GL, Mattes MJ: Mouse strains with typical mammalian levels of complement activity. *J Immunol Met* 1989, 125:147–158
  28. Webster SD, Tenner AJ, Poulos TL, Cribbs DH: The mouse C1q A-chain sequence alters  $\beta$ -amyloid-induced complement activation. *Neurobiol Aging* 1999, 20:297–304
  29. Dubois RN, Abramson SB, Crofford L, Gupta RA, Simon LS, Van De Putte LB, Lipsky PE: Cyclooxygenase in biology and disease. *FASEB J* 1998, 12:1063–1073
  30. Vane JR, Bakhle YS, Botting RM: Cyclooxygenases 1 and 2. *Annu Rev Pharmacol Toxicol* 1998, 38:97–120
  31. O'Banion MK: Cyclooxygenase-2: molecular biology, pharmacology, and neurobiology. *Crit Rev Neurobiol* 1999, 13:45–82
  32. Yamagata K, Andreasson KI, Kaufmann WE, Barnes CA, Worley PF: Expression of a mitogen-inducible cyclooxygenase in brain neurons: regulation by synaptic activity and glucocorticoids. *Neuron* 1993, 11:371–386
  33. Nam MJ, Thore C, Busija D: Effects of protein kinase C activation on prostaglandin production and cyclooxygenase mRNA levels in ovine astroglia. *Prostaglandins* 1996, 51:203–213
  34. O'Banion MK, Miller JC, Chang JW, Kaplan MD, Coleman PD: Interleukin-1 $\beta$  induces prostaglandin G/H synthase-2 (cyclooxygenase-2) in primary murine astrocyte cultures. *J Neurochem* 1996, 66:2532–2540
  35. Bauer MK, Lieb K, Schulze-Osthoff K, Berger M, Gebicke-Haerter PJ, Bauer J, Fiebich BL: Expression and regulation of cyclooxygenase-2 in rat microglia. *Eur J Biochem* 1997, 243:726–731